

## Supporting Information

### **Virus-Templated Near-Amorphous Iron Oxide Nanotubes**

Sachin N. Shah,<sup>†,‡,■</sup> Abid A. Khan,<sup>†,#</sup> Ana Espinosa,<sup>§</sup> Miguel A. Garcia,<sup>Δ</sup> Wiwat Nuansing,<sup>†</sup> Mariana Ungureanu,<sup>○</sup> Jonathan G. Heddle,<sup>‡,¶</sup> Andrey L. Chuvilin,<sup>†,◆</sup> Christina Wege,<sup>¶</sup> and Alexander M. Bittner\*<sup>†,◆</sup>

<sup>†</sup>CIC nanoGUNE Consolider, E-20013, Donostia-San Sebastián, Spain

<sup>‡</sup>Heddle IRU, RIKEN, 2-1 Hirosawa, Wako, Saitama 351-0198, Japan

<sup>¶</sup>Malopolska Centre of Biotechnology, Jagiellonian University, Gronostajowa 7, 30-387, Krakow, Poland

<sup>■</sup>Department of Chemistry, University of Hull, HU6 7RX, Hull, United Kingdom

<sup>#</sup>Department of Biosciences, COMSATS Institute of Information Technology, Park Road, Chak Shehzad, 44000 Islamabad, Pakistan

<sup>§</sup>Instituto de Ciencia de Materiales de Madrid (ICMM) Consejo Superior de Investigaciones Científicas, c/ Sor Juana Inés de la Cruz 3, Cantoblanco, 28049, Madrid, Spain

<sup>Δ</sup>Instituto de Ceramica y Vidrio - CSIC, and Instituto de Magnetismo Aplicado “Salvador Velayos” UCM\_ADIF, 28049, Madrid, Spain

<sup>○</sup>CIC biomaGUNE, E-20009, Donostia-San Sebastián, Spain

<sup>◆</sup>Ikerbasque, Basque Foundation for Science, E-48013, Bilbao, Spain

<sup>¶</sup>University of Stuttgart, Institute of Biomaterials and Biomolecular Systems,  
Pfaffenwaldring 57, D-70569 Stuttgart, Germany

E-mail: [a.bittner@nanogune.eu](mailto:a.bittner@nanogune.eu)

### **TMV coat protein cartoon model by PyMOL**

Cartoon model of one of 2130 coat proteins of TMV (pdb 2TMV), see: Namba, K.; Pattanayek, R.; Stubbs, G.; *J. Mol. Biol.* **1989**, *208*, 307. It was produced with PyMOL Molecular Graphics System, Version 1.8 Schrödinger, LLC. The leftmost part clads the internal channel, the middle part is a rather rigid four-helix bundle, and the rightmost part forms the external surface. Residues 1, 3 and 152-154 are on the right and shown as stick models. The terminal nitrogen and the exposed indole nitrogen are shown in blue while the exposed oxygen are shown in red. The pdb model does not include the last four residues, C-terminal to residue 155 which are rather flexible. They contain another hydroxyl group (Thr-158) and the carboxylate terminus. The inset shows a magnification of the region of interest with relevant amino acids labeled.

### **EM diameters**

Figure S1 shows an example of the TEM data employed to evaluate diameters. From our SEM data, we found an average diameter for mineralized TMV of (36±8) nm. The histogram shows a tail at high diameters and a cut off at 18 nm, i.e. the diameter of the naked virus (Figure S2).

### **EDX from selected sample areas**

Upon focusing the electron beam onto small areas, we obtained local EDX spectra (Figure S3). The oxygen/carbon ratio varies, and is largest for spots on mineralized TMV. The damage induced by longer exposure is visible in (D), where the top part shows the

rectangular area exposed in (A). Such damage translates into uncontrolled amounts of carbon. Similarly the amount of silicon from the substrate is hard to quantify. Details of the structure are presented in Figure S3.

### **Tobamoviruses (TMV and ToMV)**

We used wild type TMV with the mutation G154S, [ Kadri, A.; Maiß, E.; Amsharov, N.; Bittner, A. M.; Balci, S.; Kern, K.; Jeske, H.; Wege, C.]. Engineered Tobacco mosaic virus mutants with distinct physical characteristics in planta and enhanced metallization properties. *Virus Res.* **2011**, *157*, 35–46. For some additional tests we used ToMV [Kobayashi, M.; Seki, M.; Tabata, H.; Watanabe, Y.; and Yamashita, I.; *Nano Lett.* **2010**, *10*, 773-776]. A sequence alignment (Figure S4) shows that the external surfaces are chemically nearly identical. The two sequences are 84% identical, 93% homologous. Sequences were aligned using NCBI BLAST [Altschul, S. F.; Madden, T. L.; Schäffer, A. A.; Zhang, J.; Zhang, Z.; Miller, W.; Lipman, D. J. *Nucleic Acids Res.* **1997**, *25*, 3389-3402].

Figure S5 and S6 shows that exactly the same mineralization scenario as for TMV operates also for ToMV. Iron oxide-coated ToMV samples show irregular network formation during the mineralization reaction. Each ToMV is homogeneously coated; the average diameter of the rods is  $30 \pm 2$  nm. Nanoparticles of sizes below 5 nm deposited on the external surfaces of the virion, with a layer thickness of  $7 \pm 1$  nm (diameter and thickness were calculated by ImageJ software [Schneider, C. A.; Rasband, W. S.; Eliceiri, K. W., NIH Image to ImageJ: 25 years of image analysis. *Nat. Methods* **2012**, *9* (7), 671-675]. Broken ToMVs of smaller length size are also coated with iron oxide of the same

thickness. They were usually attached to longer ToMV lines. Staining the same sample with 2% phosphotungstic acid allowed us to verify that all TMV is coated; we found no bare virions (image not shown).

### **“Post-mineralization” tests**

Iron oxide particles were synthesized without addition of TMV in the reaction mixture Fe(II) / Fe(III) at pH 9. High resolution TEM image (Figure S7) show no significant crystal or polycrystalline morphologies of iron oxide. Synthesized iron oxide particles are aggregated. Formation of some very small particles is observed, which might have formed by exposure to the high-energy electron beam. In the selected area electron diffraction (SAED) pattern the inset image shows mainly the presence of amorphous iron oxide similar to that found on the iron oxide mineralized TMV. It shows absences of lattice fringes with no significant inter-fringe planes belonging to the iron oxide crystal structure.

“Post-mineralization” was achieved via the same synthesis, followed by addition of ToMV. The sample was recovered by centrifugation and purified by passage through a 100 kDa cut-off column (Amicon Ultra Centrifuge Filters, 0.5mL, 100,000 MWCO (Mol. wt. cut off), Millipore) at 17530 g (14000 rpm, Eppendorf 5417C centrifuge) for 30 min. 3  $\mu$ L of sample were loaded onto a carbon-coated copper grid, and stained with 2 % phosphotungstic acid for 1 min. We observed a very small amount of material (Figure S5), and a structure that does not correspond to our ToMV/iron oxide hybrid S6b and S6c).

### **SAED**

Figure S8 shows the SAED pattern used for the profile shown in Figure 3c. The profile was calculated by summing and averaging radial cuts through the pattern

### **Estimation of the fraction of crystalline material**

The standard sample (Figure 3a) mass was 3.5 mg, that of the sample (Figure 3b) 5.2 mg. The ratio of the biggest peak in the 100% crystalline standard to the noise in the sample spectrum is  $\approx 5$ . This means that the peak should be visible when more than  $\approx (3.5/5.2)/5 = 13\%$  of the material is crystalline.

### **SQUID-VSM magnetometry of small amounts of weakly magnetic samples**

The magnetic behavior of mineralized TMV particles was tested in a Quantum Design MPMS SQUID-VSM at 300 K. The sensitivity is  $10^{-8}$  emu, the average error was  $7 \cdot 10^{-8}$  emu. Most samples were investigated on completely diamagnetic B-doped silicon wafer pieces (4x4 mm) (see main text). Usually, it was attempted to locate the center of the sample at 66 mm of the mounting station scale, which should locate the sample exactly between the detection coils. Fine-tuning of the distance is then taken over by a fast measurement routine at zero field. However, the coils are unable to detect very small magnetic moments ( $< 10^{-7}$  emu) for zero field in this procedure. Hence we applied a small field (0.0100-0.05 T). In extreme cases, where also size and shape play a role, we resorted to manual centering by adjusting the distance in the 63-69 mm range at small fields.

A blank test of the sample rod with a piece of bare silicon wafer provided the background diamagnetism. After subtracting the linear slope of the diamagnetic moment, the magnetization is negligibly small. The coercive field is below 0.02 T, even after applying

5 T.

### **Alignment tests in external magnetic fields**

Two large  $\text{Nd}_2\text{Fe}_{14}\text{B}$  magnets (ca. 10x10x1.5 cm) were fixed with a 1 cm gap between two 10x1.5 cm sides (Figure S9), yielding a field of  $\approx 1$  T. CAUTION: Permanent magnets of this size can attract magnetic objects with very strong forces and should always be clamped. A Si wafer substrate of 4x4 mm was kept in the center between the magnets, in order to avoid the high magnetic gradients at the edges of the magnets. A 1  $\mu\text{L}$  droplet of  $\approx 0.1$  mg/mL mineralized TMV suspension was placed on the wafer, and dried in air. The sample was analyzed by SEM. The mineralized TMV moved to the right hand side of the droplet (Figure S10), an observation we never made during drying in the absence of magnetic fields. Such a “global” movement of nearly all sample material could be explained by spurious field gradients. More important is that we found no alignment with the field: SEM at increased magnification (Figure S11) showed mineralized TMV, but no orientation. In fact, the mineralized TMV formed the usual irregular network structure during synthesis. However, the mentioned field gradients should suffice to improve the quality of ferrofluids. In fact, even totally nonmagnetic pure TMV shows a huge effect [Wu, Z.; Mueller, A.; Degenhard, S.; Ruff, S. E.; Geiger, F.; Bittner, A. M.; Wege, C.; Krill Iii, C. E. *ACS Nano* **2010**, *4*, 4531].

Tests with 10-fold reduced concentration, and with sonication to break the network of mineralized TMV, under otherwise identical conditions, did not improve the result significantly, but again the sample material as a whole moved to one side (Figure S12). Obviously, the iron oxide layer, especially at the initial phase of its growth, has insufficient magnetization to induce alignment even in a rather strong field. Clearly after

the network formed, with a multitude of iron-oxygen contacts between two virions, it cannot subsequently be broken up into individual particles.

### **XPS data**

In addition to data from purified samples, we also investigated dried droplets from the synthesis suspension. They contain NaCl, but also large iron oxide particles whose properties are very similar to bulk iron oxide. These samples offer much material and thus a very good signal/noise ratio (Figure S13), but we have not considered them further because the potential presence of larger nodules (>30 nm diameter) means that also material that is not bound to TMV would be included in the analysis.

To confirm the peak energies, we tested fitting Gauss-Lorentzian curves of 30%-70% and 80%-20%. The latter gave insufficient fits, and induced shifts up to 0.3 eV in the peak position. We also tested a short ion etching to remove the top layer of the material; the results were identical.

### **EEL spectra and standards**

We recorded EELS (Figure S14) in a Cs-corrected energy-filtering FEI Titan G2 60-300. The energy resolution allows easy comparison of the Fe edge measured by XPS (main text). The O1s edge is so well resolved that tiny differences are revealed (Figure S15). Their interpretation is completely in line with the one presented in the main text: Mineralized TMV shows similarity to magnetite and maghemite, which corroborates the XPS results.



### Supporting information

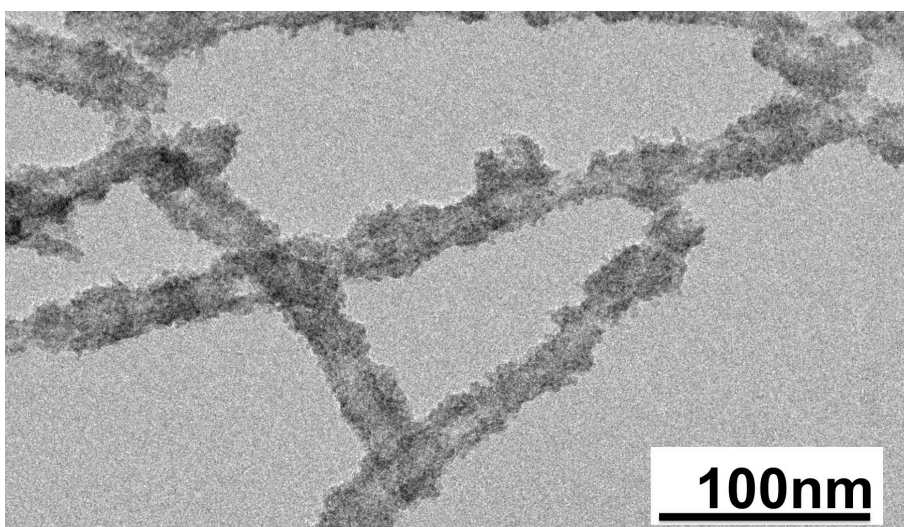


Figure S1: TEM image of iron oxide mineralized TMV. The oxide shows up as a dark gray layer, while TMV shows very weak contrast. The average coating thickness is  $\approx 5$  nm, while TMV rods measure 18 nm in diameter.

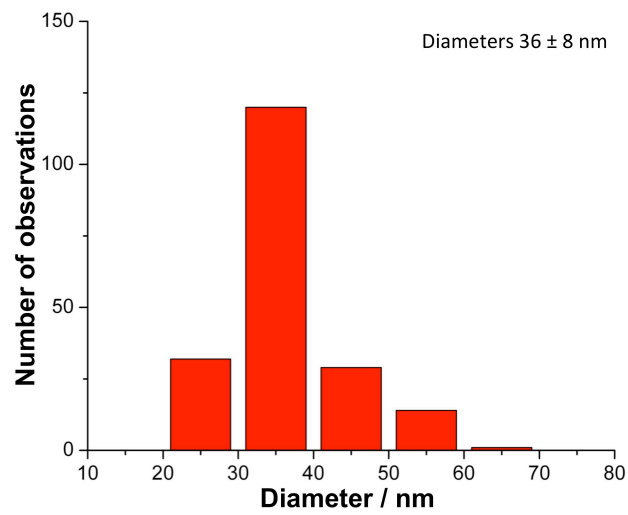


Figure S2: Distribution of the diameters of mineralized TMV. SEM data averaged from three independent experiments.

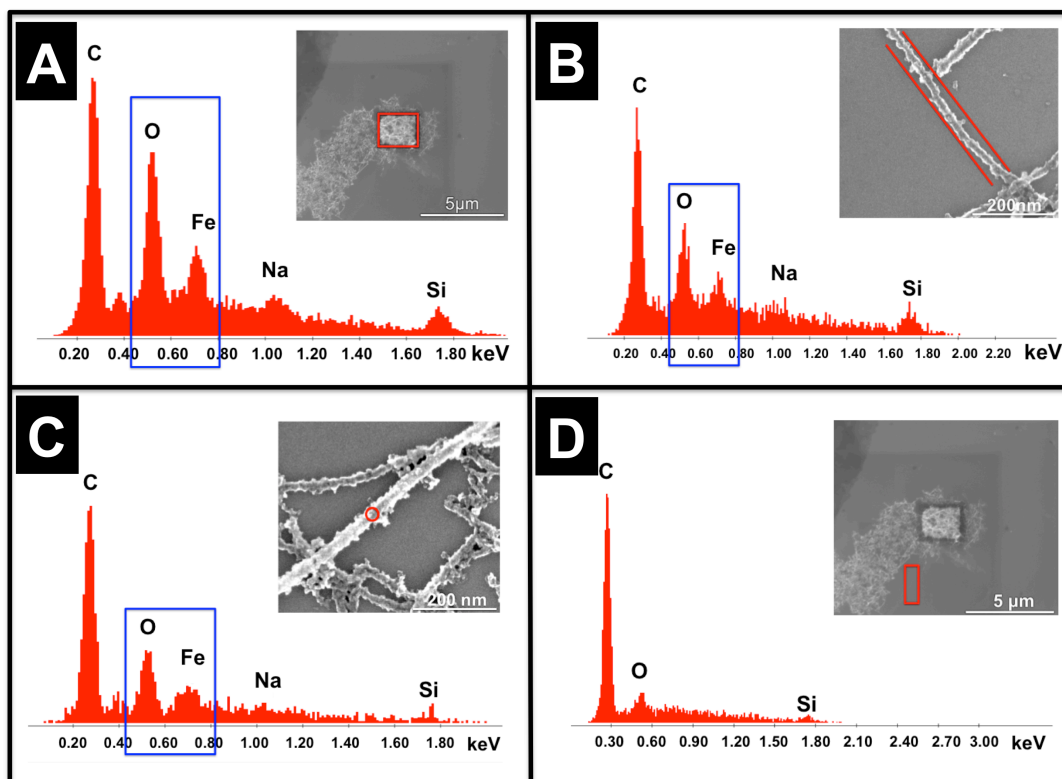


Figure S3: Local EDX spectra from selected areas. (A) large areas with mineralized TMV and bare surface spots; (B) rectangular area mainly on TMV; (C) spots exclusively on mineralized layer; (D) bare wafer surface.

	+		#		+	+	+			#	+		#	#	
	S	Y	S	I	T	P	S	Q	F	V	L	S	S	A	W
	S	Y	S	I	T	P	S	Q	F	V	L	S	S	V	W
	D	P	I	E	L	L	N	V	C	T	N	S	L	G	N
	Q	F	Q	T	Q	Q	A	R	T	V	V	Q	R	Q	F
	S	E	V	W	K	P	S	P	Q	V					
	S	Y	S	I	T	P	S	Q	F	V	L	S	S	V	W
	D	P	I	E	L	L	N	V	C	T	N	S	L	G	N
	Q	F	Q	T	Q	Q	A	R	T	T	V	Q	Q	F	
	S	E	V	W	K	P	F	P	Q	S					
	T	V	R	F	P	D	S	D	F	K	V	Y	R	N	
	T	V	R	F	P	D	S	D	F	K	V	Y	R	N	
	A	V	L	D	P	L	V	T	A	L	L	G	A	F	
	A	V	L	D	P	L	V	T	A	L	L	G	A	F	
	D	T	R	N	R	I	I	E	V	E	N	Q	A	N	
	D	T	R	N	R	I	I	E	V	E	N	Q	A	N	
	P	T	T	A	E	T	L	D	A	T	R	R	V	D	
	P	T	T	A	E	T	L	D	A	T	R	R	V	D	
	T	V	R	F	P	D	S	D	F	K	V	Y	R	N	
	T	V	R	F	P	D	S	D	F	K	V	Y	R	N	
	A	V	L	D	P	L	V	T	A	L	L	G	A	F	
	A	V	L	D	P	L	V	T	A	L	L	G	A	F	
	D	T	R	N	R	I	I	E	V	E	N	Q	A	N	
	D	T	R	N	R	I	I	E	V	E	N	Q	A	N	
	P	T	T	A	E	T	L	D	A	T	R	R	V	D	
	P	T	T	A	E	T	L	D	A	T	R	R	V	D	
	A	T	V	A	I	R	S	A	I	N	N	L	I	V	
	A	T	V	A	I	R	S	A	I	N	N	L	I	V	
	L	I	R	G	T	G	S	Y	N	R	S	S	F	E	
	L	I	R	G	T	G	S	Y	N	R	S	S	F	E	
	S	S	G	L	V	W	T	S	G	P	A	T			
	S	S	G	L	V	W	T	S	G	P	A	T			
	A	T	V	A	I	R	S	A	I	N	N	L	V	N	
	A	T	V	A	I	R	S	A	I	N	N	L	V	N	
	L	V	N	E	L	V	R	G	T	G	L	Y	N	Q	
	L	V	N	E	L	V	R	G	T	G	L	Y	N	Q	
	N	T	F	E	S	M	S	G	L	V	W	T	S	A	
	N	T	F	E	S	M	S	G	L	V	W	T	S	A	
	P	A	S												
	P	A	S												

Figure S4: Alignment of amino acid sequences of ToMV (red) [Kobayashi, M.; Seki, M.; Tabata, H.; Watanabe, Y.; and Yamashita, I.; *Nano Lett.* **2010**, *10*, 773-776] with TMV *vulgare* strain (black, UniProt ID **P69687**). Conservative, non-identical residues are indicated with "+". Non-conservative residues are highlighted with "#".

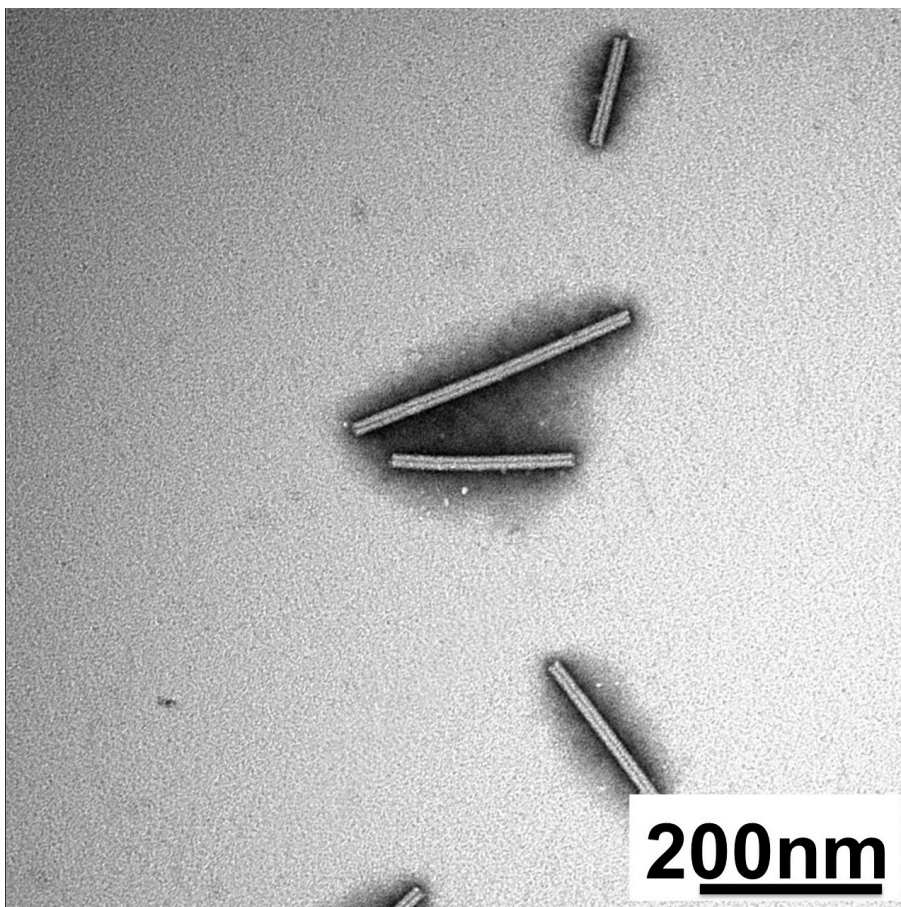


Figure S5: TEM of a stained “post-mineralization” sample. ToMV was added to a mixture of Fe(II) / Fe(III) at pH 9 at the end of the standard mineralization time (see main text). The micrograph shows uncoated ToMV. The central 4 nm channel is clearly visible.

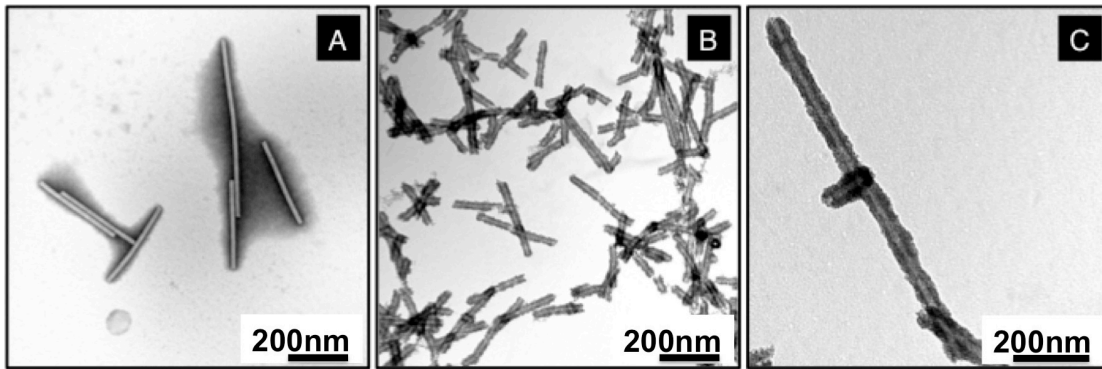


Figure S6: TEM image (A) Wild-type ToMV, negatively stained with 2% phosphotungstic acid (PTA). TEM images B and C show unstained mineralized ToMV, synthesized and purified under similar conditions as the mineralized TMV.

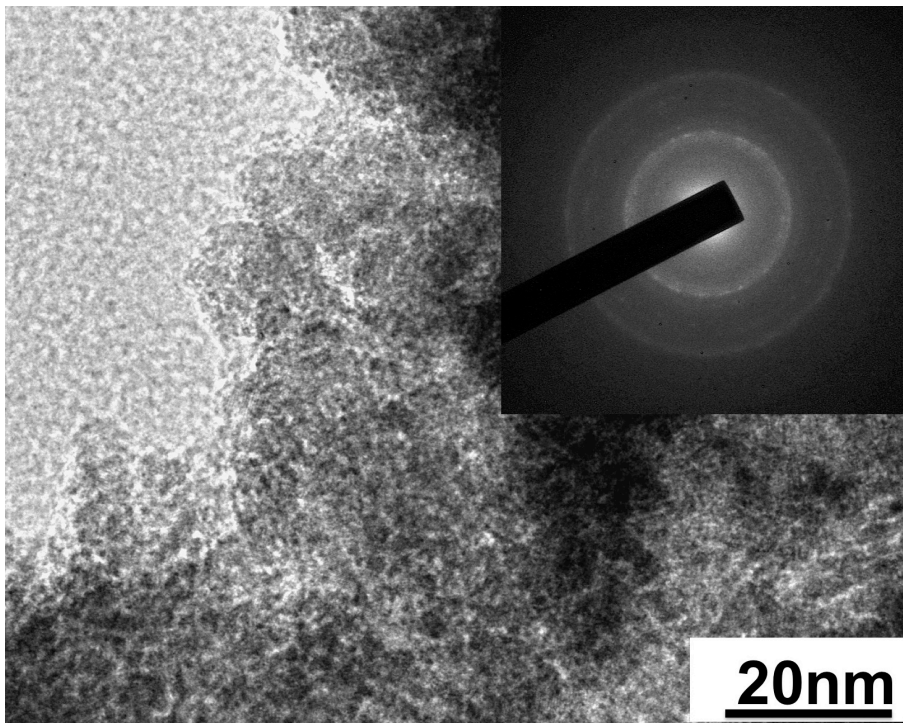


Figure S7: Iron oxide synthesis without virion addition in mixture of Fe(II) / Fe(III) at pH 9. There are no significant signs indicating formation of crystalline material. The inset shows a selected area electron diffraction (SAED) pattern of the material.

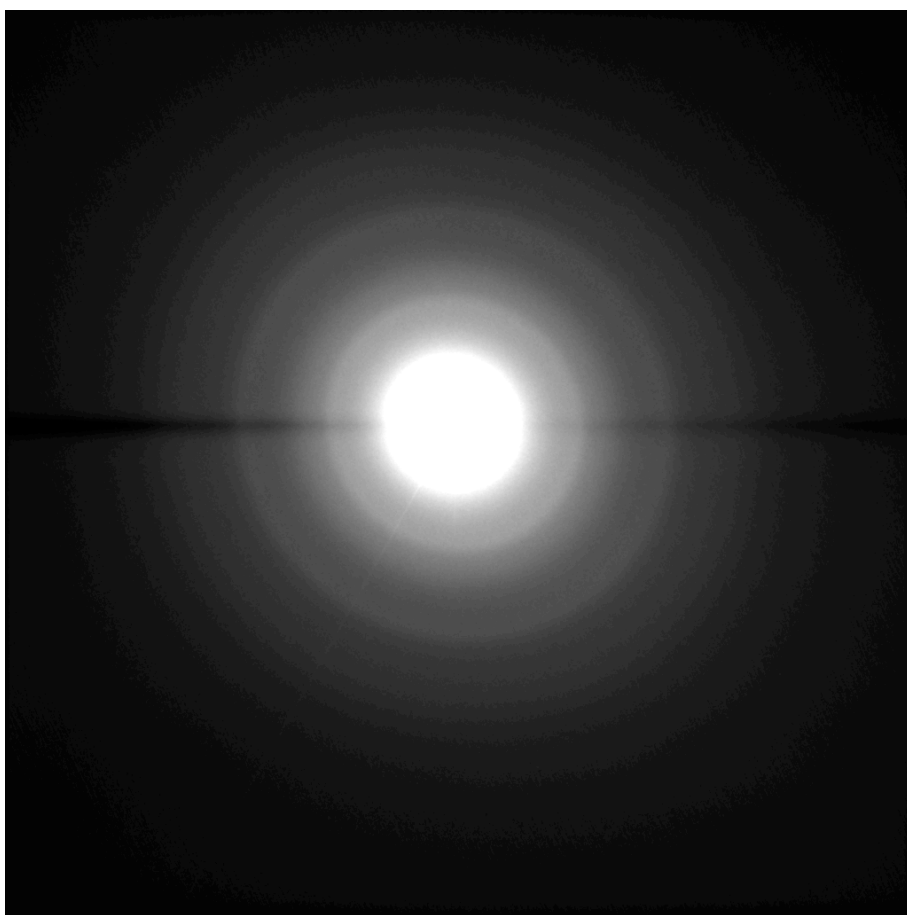


Figure S8: SAED pattern of iron oxide on TMV.



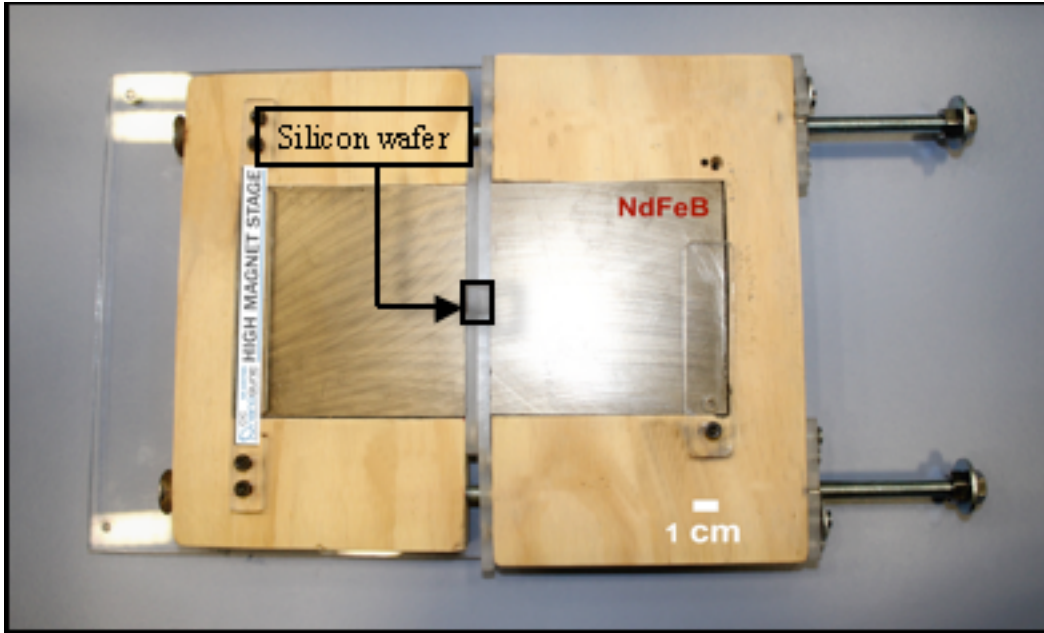


Figure S9: Magnetic stage with two  $\text{Nd}_2\text{Fe}_{14}\text{B}$  magnets. The distance between the magnets is adjusted to 1 cm, yielding a field of  $\approx 1$  T in the gap. The black square marks the location of the silicon wafer substrate for alignment experiments.

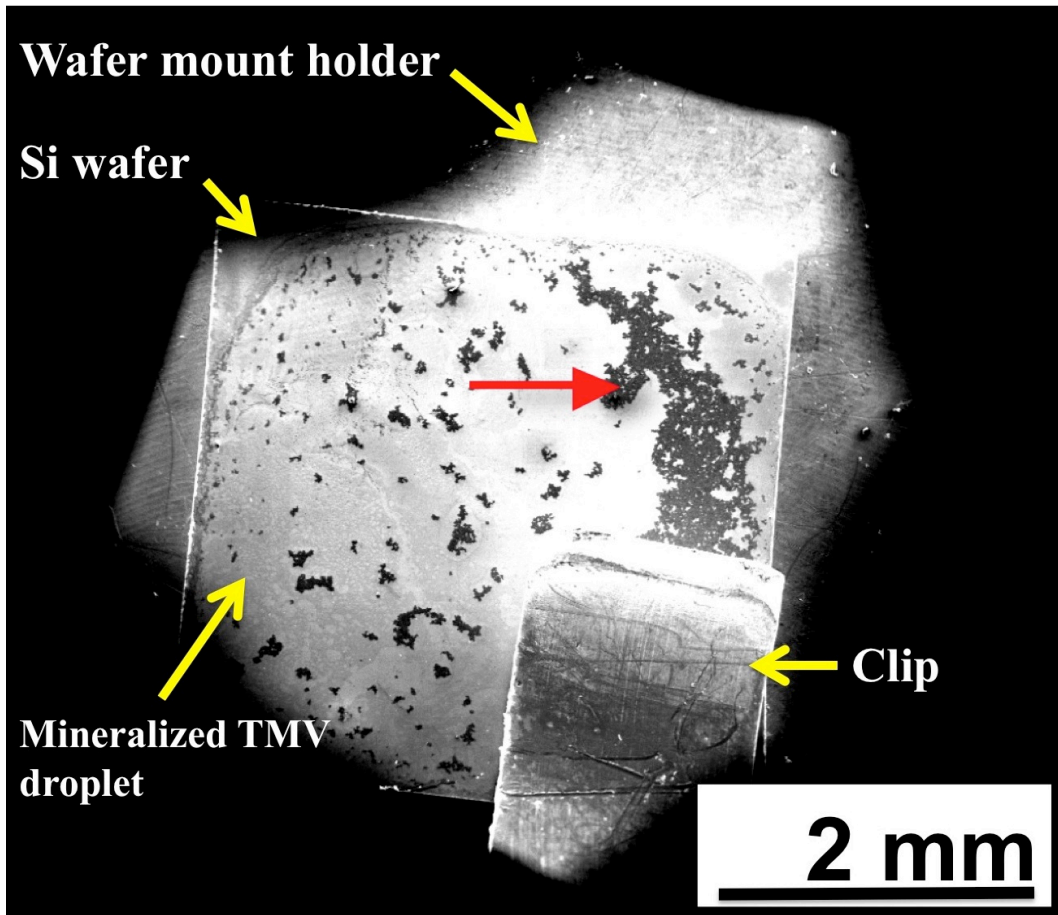


Figure S10: SEM image of a droplet of mineralized TMV, dried on a substrate (rectangular) in a strong magnetic field. The red arrows show the direction of the magnetic field (gradient). The substrate is surrounded by bright reflections from the SEM holder. The rectangular feature on the lower right is a clip.

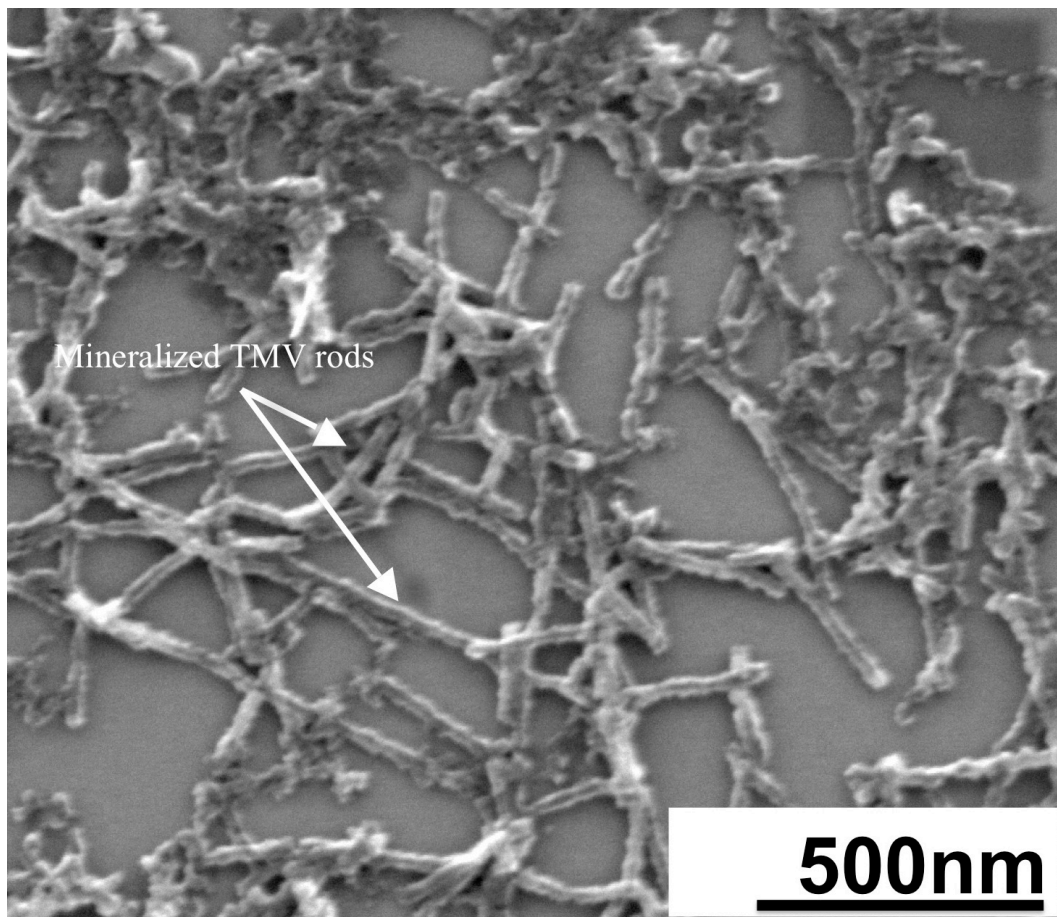


Figure S11: SEM image. The network of mineralized TMV shows no clear alignment, despite the presence of a strong magnetic field.

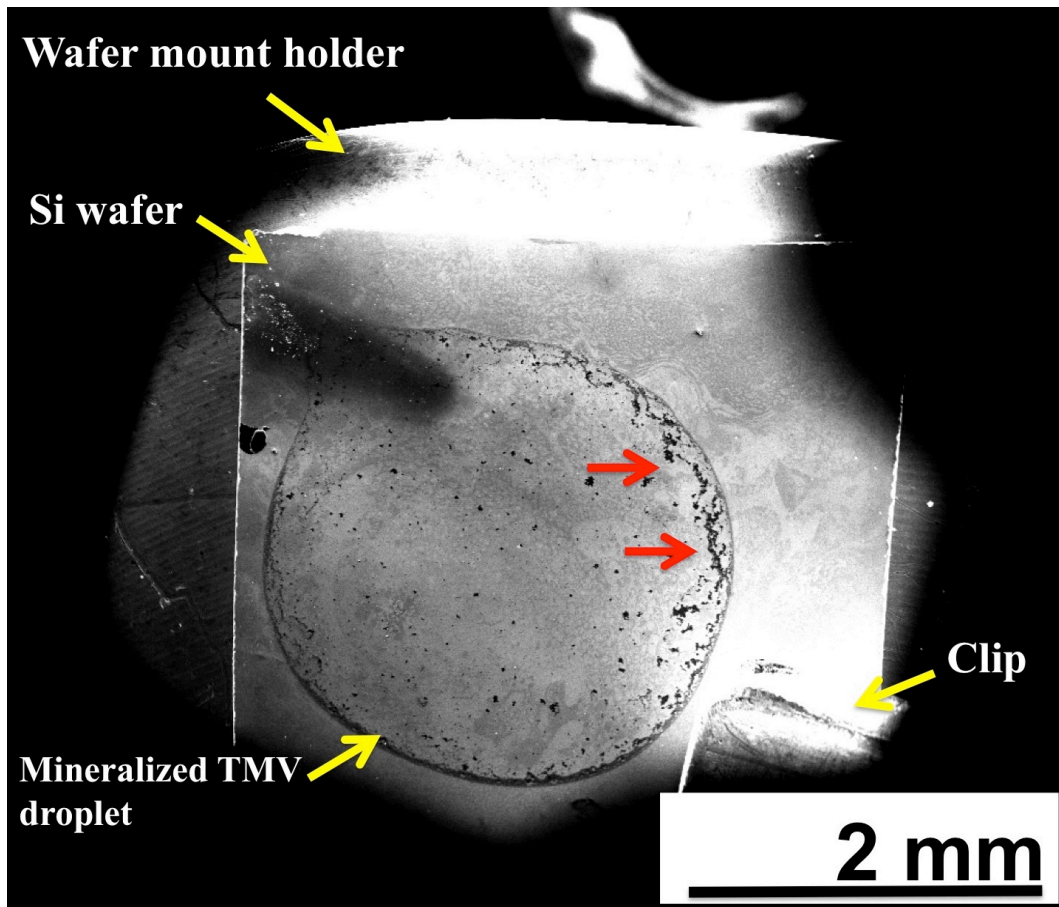


Figure S12: SEM image of a droplet of diluted mineralized TMV after sonication and placement on a substrate (rectangular). The red arrows show the direction of the magnetic field (gradient). The substrate is surrounded by bright reflections from the SEM holder. The feature on the lower right is a clip.

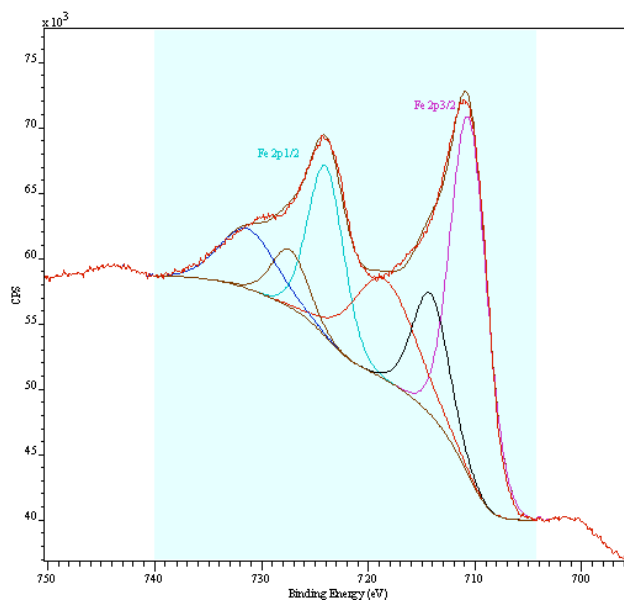
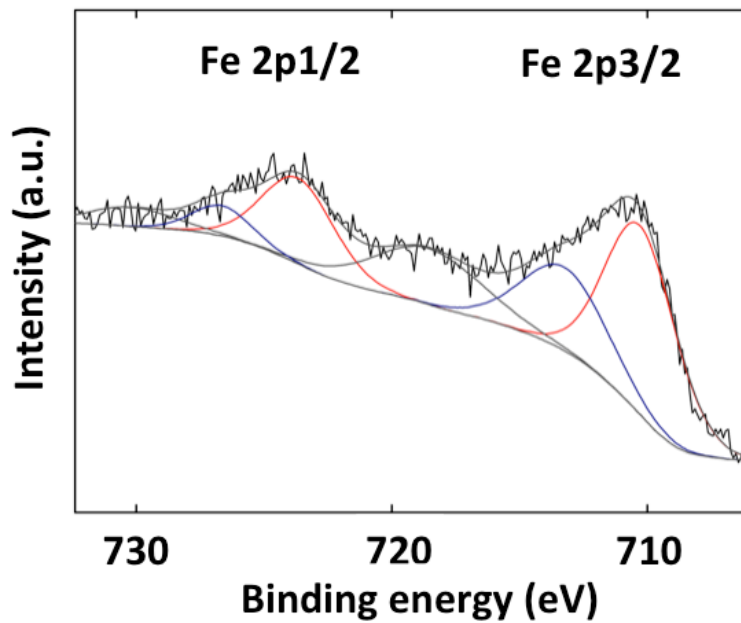


Figure S13: XPS of mineralized and purified TMV. Detail of the Fe 3p region with a fit of six components. Lower panel: Unpurified sample, the much larger amount of material reduces the noise.

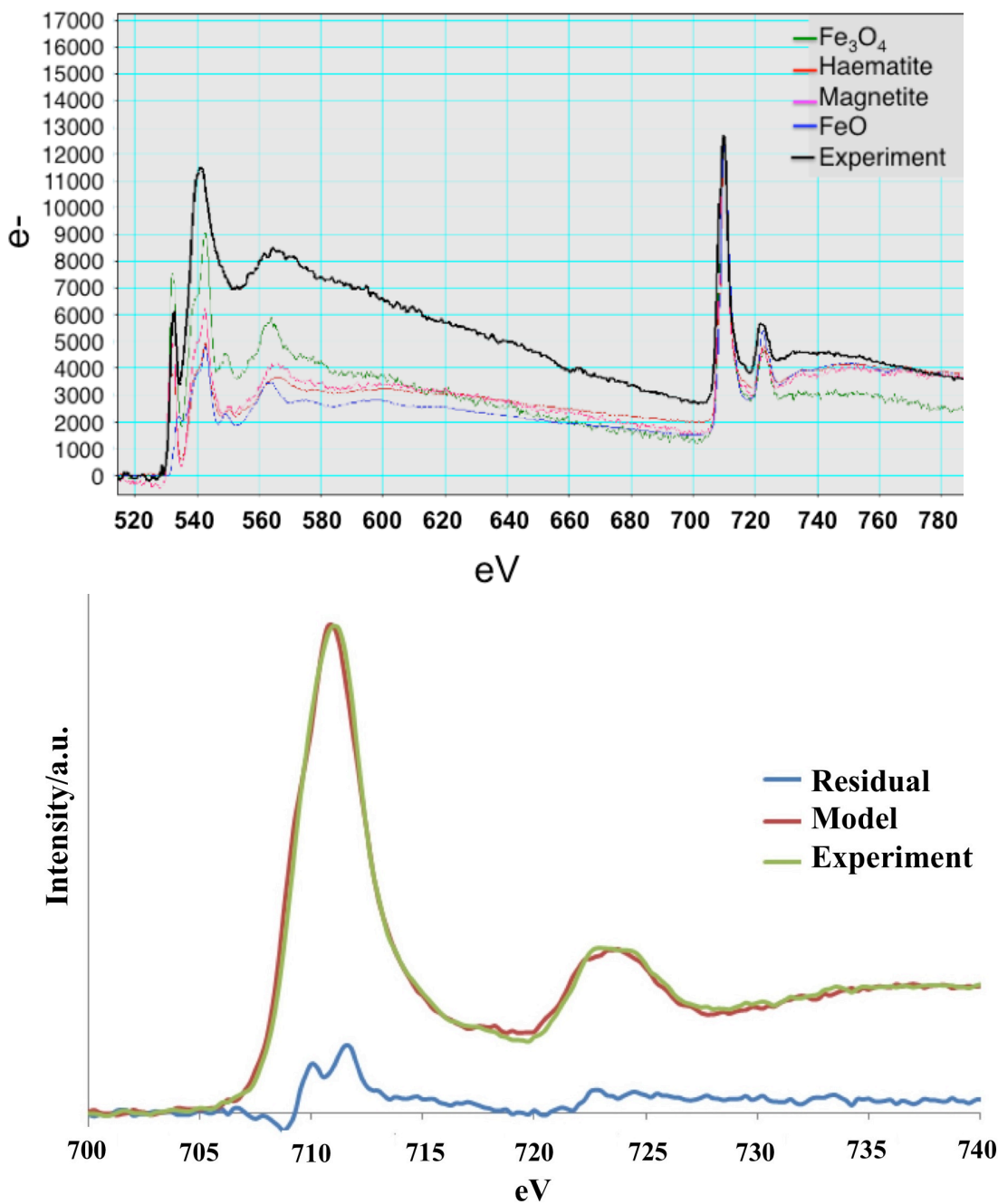


Figure S14: EELS of standard powder samples, and of mineralized TMV. All spectra were recorded on similar TEM grids, under identical settings. The Fe edge compares very well with the XPS results. Lower part: Green, detail of the Fe L edge, red, sum of modeled  $\gamma$ -Fe<sub>2</sub>O<sub>3</sub> and FeO, ratio 2:1, blue, difference between red and green traces. As seen by the ratio 2:1 of Fe(III) and Fe(II), mineralized TMV shows similarity to magnetite, which corroborates the XPS and XAS results.

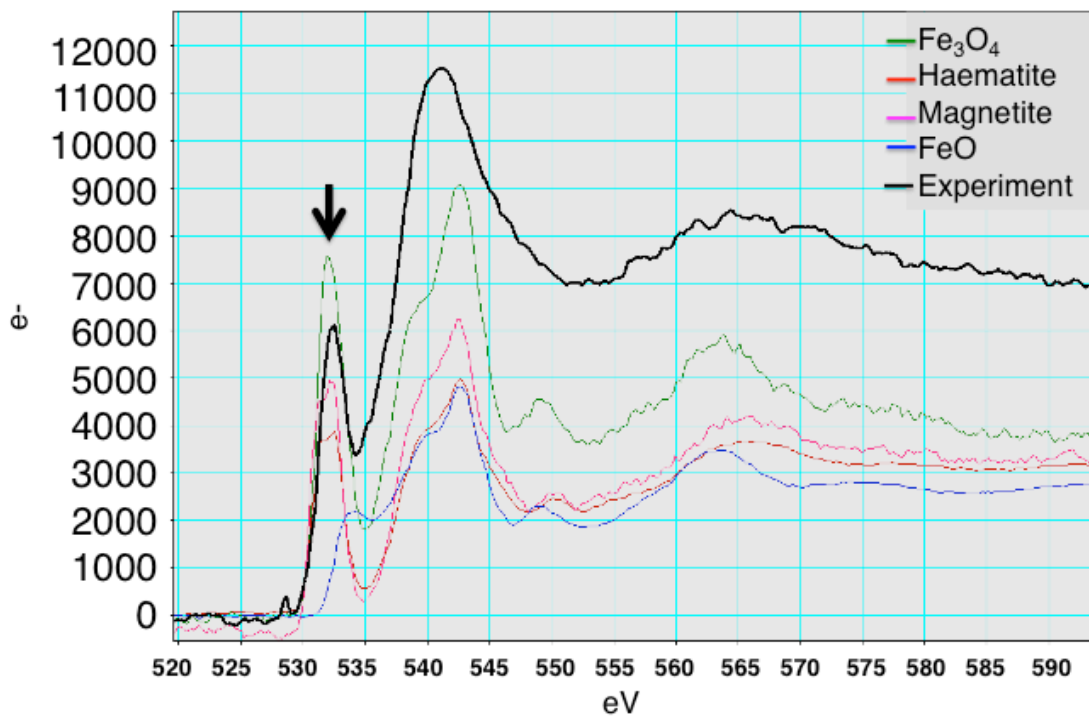


Figure S15: EELS at the O1s edge shows very small, but characteristic differences between the samples.